This is a post-peer-review, pre-copyedit version of an article published in Biogeochemistry. The final authenticated version is available online at: https://doi.org/10.1007/s10533-019-00579-0

Title: Carbon dioxide fluxes of air-exposed sediments and desiccating ponds

Authors: Kenneth Thorø Martinsen[1], Theis Kragh[1], Kaj Sand-Jensen[1]

[1]Freshwater Biological Laboratory, Biological Institute, University of Copenhagen, Universitetsparken 4, 3rd floor, 2100 Copenhagen, Denmark

Corresponding author: Kenneth Thorø Martinsen, +45 60709007, kenneth2810@gmail.com

Keywords: ponds, air-exposed sediments, CO_2 efflux, ecosystem metabolism

Acknowledgments: We are thankful for grant support from COWIfonden and the Carlsberg Foundation (CF14-0136) to Kaj Sand-Jensen to the study of environmental and biological dynamics in ponds. We thank the two anonymous reviewers for their constructive comments which helped improve the manuscript.

ORCHID:

Kenneth Thorø Martinsen 0000-0001-8064-513X

Theis Kragh 0000-0002-9760-2571

Kaj Sand-Jensen 0000-0003-2534-4638

Abstract:

Ponds are active components of the global carbon cycle processing and emitting carbon dioxide and methane to the atmosphere. These common habitats frequently experience seasonal water table variations resulting in periodically air-exposed sediments. However, the influence of these events on both the system scale carbon balance and in-pond environmental conditions remains poorly studied. We took advantage of an extraordinarily warm and dry summer to quantify the CO_2 efflux from air-exposed sediments and water surfaces in desiccating ponds on Öland, Sweden. Simultaneously, we modelled metabolism and measured environmental variables within the ponds. We found that air-exposed sediments had high CO_2 effluxes greatly exceeding that from the water surfaces. Sediment water content influenced the temperature and strongly regulated the CO_2 efflux gradually approaching zero as water evaporated.

Within the desiccating ponds, respiration was generally higher than gross primary production, but was lower compared to the same ponds with higher water table. These findings highlight the role of periodically air-exposed pond sediments as sites of highly active carbon processes. Not only is this important for the system-scale carbon in ponds, but it may also influence the destiny of buried carbon in lakes subject to climate changes. The environmental conditions within desiccating ponds, most notably high water temperatures and poor oxygen conditions, further iterate the dynamics and extreme nature of ponds.

Introduction:

Inland freshwater lakes are hotspots in the global carbon cycle (Raymond et al. 2013; Tranvik et al. 2009). They process large amounts of organic carbon that are imported, exported, buried in the sediments or decomposed and emitted as CO_2 (Cole et al. 2007; Staehr et al. 2010). The high abundance and combined area of ponds (Downing et al. 2006; Verpoorter et al. 2014) and their high CO_2 and CH_4 emissions (Holgerson and Raymond 2016) make them especially important components of carbon cycling of inland waters. While carbon conversion processes and balances have been intensely studied in water and inundated sediments, the shallow zone periodically drying out and being rewetted has received little attention (Jin et al. 2016; Schiller et al. 2014). On a global scale, periodically inundated sediments may emerge as a significant window of carbon emissions as 0.81 million km^2 (0.54 % of the global land area) is seasonally dry compared to the 2.78 million km^2 permanent freshwater bodies (Pekel et al. 2016). Seasonal air exposure of aquatic sediments may increase organic degradation and stabilise sediments and, subsequently, make them more suitable to rooted plant growth when re-inundated (Barko and Smart 1986; Baastrup-Spohr et al. 2016; Sand-Jensen and Møller 2014). This motivated us to study the pond ecosystem processes during desiccation and the drivers of the CO_2 efflux from aquatic sediments following air exposure. We focused our study on small ephemeral ponds on Öland, Sweden where pond sediments had become exposed to air due to the early onset of an extreme summer drought during 2018.

Water level fluctuation in lakes is a natural and essential phenomenon for many organisms (Wantzen et al. 2008). Amphibians and large invertebrates are characteristic of ephemeral ponds (Griffiths 1997; Williams 1997). They leave the water or survive in the sediments when the ponds dry out and they benefit from the loss of predatory fish during desiccation (Hecnar and M'Closkey 1997). Likewise, amphibious plant species forming green shoots and leaves adapted to either emergence or submergence obtain a competitive advantage compared with obligatory aquatic or

terrestrial plants (Sand-Jensen et al. 1992). Small, shallow ponds are often isolated systems whose water levels are highly dependent on the shifting balance between precipitation and evaporation (Sand-Jensen et al. 2015). Consequently, seasonal water level variations may result in drastic changes in the area of ponds and, thus, the distribution between inundated and air-exposed sediments (Christensen et al. 2013; Martinsen et al. 2019). From temporary streams, it is reported that the CO_2 efflux from air-exposed sediments is comparable to, or in some cases higher, than the efflux from the flowing waters (Gómez-Gener et al. 2016; Gómez-Gener et al. 2015; Schiller et al. 2014). Reservoirs are another habitat with large variations in water level, in which CO_2 effluxes during transition to air-exposure or inundation need quantification (Jin et al. 2016; Kosten et al. 2018). The organic carbon burial in reservoir sediments is often high (Mendonça et al. 2017) just like in nutrient-rich ponds (Downing et al. 2008; Taylor et al. 2019). What happens to stored sediment carbon upon air exposure is important for the resulting carbon budget and this is usually ignored (Prairie et al. 2018). Temporary ponds during the dry phase also have high CO_2 emission rates resembling those of upland soils (Obrador et al. 2018). Studies on the regulation of the CO_2 efflux from natural soils suggest a primary influence of soil temperature, moisture and net primary production of the vegetation cover forming the organic substrates for microbial degradation (Lloyd and Taylor 1994; Raich and Schlesinger 1992). It is likely that the same regulation of emission rates is also relevant for temporarily air-exposed aquatic sediments as recent investigations have found positive influences of organic matter, temperature and water content (Catalán et al. 2014; Obrador et al. 2018). Aquatic sediments covered by submerged vegetation will experience plant senescence during desiccation, thereby forming easily degradable organic matter. Air exposure of aquatic sediments, both bare and vegetated, will increase the oxygen supply to organic degradation, which may stimulate CO_2 emission (Baastrup-Spohr et al. 2016; Weise et al. 2016). Gradual loss of sediment pore-water may reduce microbial degradation as desiccation includes deeper layers, and minute pores and water films on particles (Fromin et al. 2010). Within a broad range, sediment temperatures may simply stimulate microbial processes as long as high temperatures (e.g. > 30 °C), which cause increasing denaturation of proteins and inhibition of membrane function, do not occur (Sand-Jensen et al. 2007).

The abundant, shallow ponds on Öland's Alvar are dominated by charophytes, which grow rapidly during spring to reach a high cover (up to 100%) and biomass (up to 450 g organic DW m^{-2}; Martinsen et al. (2017)). The dense charophyte canopy promotes strong daytime stratification followed by nocturnal convective mixing (Andersen et al. 2017b). The ponds exhibit high rates of gross primary production (GPP) and respiration (R) and

positive net ecosystem production (NEP; GPP-R > 0) during the growth season (Martinsen et al. 2017). During dry periods, the water column becomes compressed and the charophyte canopy may breach the water surface. This development is likely to influence the ecosystem metabolism by impairing the canopy structure, promoting high temperatures and reducing horizontal mixing (Christensen et al. 2013). During progressive desiccation, the pond may enter a stage where charophyte senescence dominates system scale processes (R > GPP). We wanted to quantify the processes both within the pond and on the dried-out pond sediment bed in order to evaluate the drivers that are likely to influence the fate of the plant biomass build-up during spring and early summer.

In order to fulfil those objectives, we measured the CO_2 flux from air-exposed sediments and pond water surfaces and calculated ecosystem metabolism in multiple ponds during summer in 2017 and 2018. In Scandinavia, the 2018 summer was particularly warm and dry, which allowed us to investigate ponds which had recently dried out or were in the process of desiccation. We hypothesised that: 1) Air-exposed sediments are more active sites of CO_2 emissions compared to inundated areas, and 2) charophyte photosynthesis is reduced and outweighed by respiration as the ponds gradually dry out and the canopy is compressed in a shallow water column.

Methods:

The investigated sites are located on Öland, Sweden. Ponds numbered 1 to 5 are located on Räpplinge Alvar whose ecosystem metabolism has previously been examined (Martinsen et al. 2017). This study also includes data from Pond 6 (57.115157 °N, 16.896897 °E), located close to the west coast of Öland, and Pond 7 (56.822675 °N, 16.611683 °E), which is located in a quarry just north of the five Alvar ponds with similar environmental characteristics (Fig. 1). The Alvar is a calcareous grassland landscape characterised by sparse vegetation on thin soil layers (5-10 cm) covering the limestone bedrock. The ponds are located in limestone quarries abandoned approximately 30 years ago. The ponds are nutrient poor (< 5 μg PO_4^{3-}-P L^{-1}, < 30 μg NH_4^+-N L^{-1} and < 20 μg NO_3^--N L^{-1}) with very clear water and dominated by charophytes (Martinsen et al. 2017). The common charophyte species are: *Chara aspera*, *Chara hispida*, *Chara subspinosa and Chara aculeolata*. The pond water levels show large variations through the year but are usually water-filled during early summer (i.e. June). We examined the ponds during June 2017 and 2018 with 2018 being an especially dry and warm summer (Table 1).

Environmental variables

In the ponds, data loggers mounted on steel pegs measured oxygen (one logger in each pond; MiniDOT, PME, Vista, CA, USA), water temperature (two-five loggers in each pond, HOBO UA-002-64 Onset Computers, Bourne, MA, USA, accuracy of ± 0.53 °C) as well as pH (only Pond 4 and 5, pHTemp2000 MadgeTech data logger with an Omega pH electrode). The temperature sensors were distributed vertically down through the water column at approximately equal distances. Oxygen sensors were calibrated at 0 % (water bubbled with N_2) and 100 % air saturation. Meteorological variables (wind speed and wind gust: HOBO S-WSET-A, relative humidity and air-temperature: HOBO U23 Pro v2, PAR: HOBO S-LIA-M003) were measured at a central station near Pond 4 at 2.5 meters height. In 2018, atmospheric pressure was measured at the meteorological station (HOBO U-20-001-04). In-pond and meteorological variables were measured every 10 minutes. In 2017, hourly values were obtained from Kalmar airport 25 km away (SMHI 2018). We also obtained daily measurements of air temperatures from Kalmar and precipitation from Skedemosse (8.5 km away) to compare the summer in 2017 and 2018 with long term averages.

Pond bathymetry for the new sites (Ponds 6 and 7) supplemented existing bathymetries for Ponds 1-5 (Martinsen et al. 2017) in order to calculate the mean depth (z_{mean}, m) and surface area (m^2). New bathymetries were determined from manual measurements of water depth (accuracy 0.5 cm) along regularly spaced transects. Surface area was determined using drone photography (Phantom 3 Professional, DJI, China) with 50 % overlap in both x and y directions. The pictures were assembled using the *photomerge* tool (auto), calibrated and the area was measured (Photoshop CC, Adobe, USA). Water depths in each pond were measured manually on a daily basis at a fixed position to track fluctuations of the water level.

Measurement of water CO_2 dynamics

The CO_2 efflux was measured from the pond water surfaces using plastic domes equipped with CO_2 mini-loggers (ELG CO_2 logger, SenseAir, Sweden). We used the floating chambers described in Bastviken et al. (2015) with air volumes of 7.5 and 5.6 L covering surface areas of 0.08 and 0.033 m^2, respectively. One chamber deployed on Pond 4 was modified with an air-pump and timer; it permitted periodic evacuation of the chamber headspace in order to provide frequent measurements of the gas flux with vent and pause durations of 10 and 30 minutes respectively (Martinsen et al. 2018). All chambers were covered with aluminium tape to minimise internal heating. Measurements on the water surface

lasted at least 20 minutes, while logging the CO_2 mixing ratio (ppm) at five minutes intervals. The mini-loggers were calibrated in CO_2-free air (N_2) following the manufacturer's instructions. We calculated the flux (F, reported as mmol m^{-2} h^{-1} with positive values being fluxes from water surface or sediment to atmosphere) as:

$$F = \frac{dCO_2}{dt} \frac{P_{amb} V}{R_{gas} TA} \text{ (eq. 1)}$$

The first term ($\frac{dCO_2}{dt}$¿ is the rate of change in CO_2 over time in the floating chamber, P_{amb} is the ambient atmospheric pressure (atm), V is the chamber volume, R_{gas} is the universal gas constant (m^3 atm K^{-1} mol^{-1}), T is the ambient temperature (K) and A is the chamber area in contact with water or sediment. For measurements on the water surface, we discarded measurements of CO_2 concentration *versus* time yielding a slope with a R^2-value below 0.9. In addition to the gas flux measurements, floating chambers (7.5 L and 0.08 m^2) were left on the water surface in Ponds 4 and 5 to equilibrate with the surface water CO_2 partial pressure. Waterside CO_2 partial pressure was also determined from pH, alkalinity and temperature in Ponds 4 and 5 following Weyhenmeyer et al. (2012). Alkalinity was determined by acidimetric titration with 0.1 M HCl (Gran 1952). The investigated ponds are generally alkaline with alkalinity > 1 meq. l^{-1}, high pH values (7.5-9.8) and low in dissolved organic matter which should result in low bias when estimating CO_2 partial pressure from alkalinity and pH (Abril et al. 2015).

Measurement of CO_2 flux and characteristics of air-exposed sediments

Measurements on air-exposed sediments were performed at seven sites surrounding Pond 1, 4 and 5 and covered different desiccation gradients during summer 2018 (Table 1 and 2). These sites are water covered at normal water supply levels, however, periods with low precipitation and high evapotranspiration may render them periodically air-exposed. We used chambers identical to the ones used for water surface measurements with a volume of 5.6 L, covering an area of 0.033 m^2 and equipped with an internal fan taken from a computer. Measurements were performed in duplicate, lasted 5 minutes, while logging the CO_2 mixing ratio (ppm) every 30 seconds. Subsequently, the initial 90 seconds and the last 30 seconds of the recordings were discarded to avoid artefacts of setting up and handling the chambers. Measurements with a response not exceeding sensor accuracy (<5 ppm change, 18 % of measurements) or artificial high initial partial pressure exceeding that of the atmosphere (4 % of measurements) were discarded.

Discarded measurements stem almost entirely from very dry sediments with emissions rates very close to zero. Following this selection, the average values were used in further analysis. Temperature sensors (HOBO UA-002-64) were deployed at 2-4 cm depth in the sediments. Measurements in Ponds 2 and 3, which had completely dried out and are devoid of any visible water, supplemented these measurements. Moreover, on Pond 5, the CO_2 flux was measured at 1 m intervals away from the water edge (0-8 m). For each measurement, we sampled a sediment core (3 cm height, tube diameter 22 mm) and analysed water content (%) as weight loss after drying and loss on ignition after four hours at 550 °C and 950 °C (LOI_{550} and LOI_{950}) to quantify the organic matter and carbonate content, respectively. We determined organic matter and carbonate content of the 3-cm thick core samples and reported the content as g m^{-2} per 1-cm sediment layers after dividing by 3. At each site, we also determined the average sediment depth (height of sediment above bedrock) from eight point measurements placed at random using a measuring stick. The turnover time for each site was calculated as the carbon pool size divided by the carbon CO_2 efflux rate. The carbon pool was calculated as the product of the sediment depth and LOI_{550} multiplied by 0.4 (the approximate proportion of carbon in organic matter).

Whole-system metabolism

Pond metabolism (GPP, R and NEP) was estimated using an inverse modelling approach to model free-water oxygen metabolism. Changes of oxygen concentrations between successive measurements are a result of GPP, R and air-water gas exchange (Solomon et al. 2013). We used the method described in detail in Martinsen et al. (2017) with one difference. Due to the noise and spiky nature of the oxygen data in the desiccating ponds, it was not possible to model the metabolic parameters on a daily basis. This failure was due to unsatisfactory discrepancies between modelled and observed oxygen concentrations. Instead, we used data from the entire period (three to five days) to estimate the metabolic parameters. This alleviated some of the problems associated with the observed noise because events like sudden nocturnal increases in oxygen on some days will not force the model to collapse or give unrealistic estimates. However, this approach requires the assumption that the functional metabolic parameters are relatively constant over three-five days which our previous investigations suggest is reasonable (Christensen et al. 2013; Martinsen et al. 2017). In short, oxygen dynamics were modelled by estimating three free parameters which describe GPP (two) and R (one). GPP is parameterized by a light-saturating function (Jassby and Platt 1976), R as a function of water temperature with a Q_{10} of 2 (Jørgensen and Bendoricchio 2001) and gas exchange determined using a relationship previously established by

floating chamber measurements in Pond 4 (Kragh et al. 2017). Mixed-layer depth was determined from water temperature profiles (Read et al. 2011). When only two water temperature sensors were present, mixed-layer depth was set equal to half the total depth when the difference between the sensors exceeded 1 °C. Confidence intervals (95 %) of the parameter estimates were calculated using a bootstrap procedure with 999 iterations. Volumetric rates (g O_2 m^{-3} day^{-1}) were converted to rates per surface area by multiplying with mean water depth..

Statistical analysis

To compare CO_2 effluxes from different habitats, we distinguished between water-saturated sediment with degrading water-saturated charophytes and bare desiccated sediments of mainly clay. Sediments were divided into wet (>50 % water content) and dry (<50 %). This threshold represents the mid-point of the investigated habitats which ranged from completely dry to water logged and was only used for the initial exploration. Differences between habitats were examined using a Kruskal-Wallis test followed by Dunn's test for multiple comparisons ($\alpha = 0.05$).

To examine drivers of CO_2 efflux from air-exposed sediments, we used linear mixed-effect modelling (Bates et al. 2015) and included "site" as a random variable (intercept) acknowledging that observations within sites are more similar than observations between sites (Bolker et al. 2009). The response variable (CO_2 efflux) was ln-transformed to improve normality of the residuals. All possible models were evaluated within an information theoretical framework using the Akaike Information Criterion (AIC) corrected for small sample sizes (AIC_c; Burnham and Anderson (2002)). To evaluate model fits, we calculated R^2_{marg} and R^2_{cond}, which is the variance explained by fixed factors alone and both fixed and random factors, respectively, using the "MuMIn" package in R (Barton 2018; Nakagawa and Schielzeth 2013). All data analysis was performed in R (R Core Team 2018).

Results:

Climate conditions

The 2018 summer (June, July and August) was 2.7 °C warmer, while the 2017 summer was only 0.2 °C warmer than the long term (1980-2010) summer average of 16.2 °C for the area. The precipitation followed a similar pattern with a summer sum of 106 mm in 2018 and 192 mm in 2017 compared to the long term average of 162 mm. Of the 106 mm precipitation in the summer 2018, 62 mm fell during the last two days of August, long after our measurement campaign.

The data highlights the extreme heat and drought experienced in 2018. The meteorological measurements at the investigated sites during the week long measurement campaigns in June 2017 and 2018 showed only subtle difference (Fig. S1). The daily decrease of water levels was very similar (0.5-1 cm d^{-1}) during both June periods. Thus, the desiccation of the investigated ponds in 2018 was the result of a prolonged period with higher air temperatures and lower precipitation than average before and under the June campaign.

CO_2 efflux and temperature dynamics in air-exposed sediments

Gradual desiccation of the investigated ponds was especially pronounced during summer 2018 and allowed measurements and evaluation of the importance of CO_2 effluxes from air-exposed aquatic sediments. Compared to CO_2 effluxes across the water surface, habitats at different stages of desiccation showed high effluxes (Table 2, Fig. 2). Air-exposed sediments with high water content and sites with decaying *Chara* showed the highest CO_2 effluxes. This pattern was also evident along a natural hydrological gradient with both CO_2 efflux and water content in the sediments decreasing extensively with distance from the water edge (Fig. 3). Measured CO_2 effluxes ranged from high rates close to the water edge (10.8 mmol m^{-2} h^{-1}) to undetectable as water content approached zero in sediments far from the water edge.

High-frequency measurements of temperature in the air-exposed sediment revealed substantial differences between habitats (Fig. 4). Sediment temperatures followed the same sinusoid diel curve as air temperatures but were generally higher (sediment mean 19.6 °C, air mean 17.5 °C). The sediments heated differently during the day with dry sediments reaching the highest temperatures (16.2-31.9 °C) and wet sediments being cooler (14.6-25.8 °C). Temperatures within decaying *Chara* (15.1-26.8 °C) were in between those in bare wet and dry sediments.

Linear mixed-model of CO_2 efflux from air-exposed sediments

Using the measured sediment characteristics, we modelled the CO_2 efflux from the air-exposed sediments. The best model contained sediment temperature, water content (including a squared term), LOI_{550} and LOI_{950} with a R^2_{marg} value of 0.84 (Table 3). The fit improved significantly by including a squared term for water content (Fig. 5). A model with only temperature and water content had an R^2_{marg} of 0.41 (AIC_c = 93.9). Adding a squared term of water content to this model increased the R^2_{marg} to 0.74 (AIC_c = 80.0) thus performing almost as good as the best model (Table 3). The non-

linear response to water content is likely due to the sites with drying *Chara*, which are saturated with water to a degree where the CO_2 efflux is hampered. In contrast to expectations, LOI_{550} and LOI_{950} had a negative and positive effect, respectively, on the CO_2 efflux. The results emphasise the predominant influence of water content on the CO_2 efflux rates in the air-exposed sediments.

In-pond consequences of desiccation

Within the ponds, we observed marked consequences of the dry summer and low water table in 2018. In the exposed Alvar ponds, the water surface receded and left much of the *Chara* canopy compressed at the surface, which resulted in high water temperatures (daily maximum 23.4-29.3 °C) and inhibition of photosynthesis. As the photosynthetic capability was reduced, respiratory processes also declined, but exceeded photosynthesis. In turn, this development invoked low oxygen saturation and frequent anoxic events in the water column (Table 4, Fig. 6). During daytime, photosynthesis raised pH to above 9 (maximum 9.6) and caused undersaturation of dissolved CO_2 (Fig. 6). This apparent undersaturation was also evident from manual measurements of pH and alkalinity. The permanent floating chambers equilibrating with the waterside likely had CO_2 partial pressure delayed in time because the metabolic rates greatly exceeded the rates of gas transfer. In Pond 4, the CO_2 efflux was lowered and on one occasion went from nocturnal emission to invasion in the water at noon at low surface water CO_2 because of CO_2 depletion by photosynthesis (Fig. 7). However, at low light and during night-time, respiration dominated and resulted in extensive CO_2 oversaturation uncommon for deeper ponds (Andersen et al. 2017a). Concurrent manual measurements of water surface CO_2 efflux revealed emissions at all times in Ponds 1 and 5 (Table 5). The observed diel O_2 curves are highly irregular with spikes during days of low water levels in 2018, and are markedly different from the regular sinusoid O_2 curves in previous years with deeper water (2015, 2016 and 2017; Martinsen et al. (2017)).

Whole system metabolism was calculated during desiccation to compare rates from summer 2018 with measurements in previous years. It is evident that both GPP and R were low during very dry periods of low water levels (summer 2018, Table 4). Moreover, NEP values became negative or zero during desiccation compared to positive NEP in previous summers with deeper water. The dominance of O_2 consumption compared to production is also supported by the pronounced and consistent O_2 undersaturation relative to atmospheric equilibrium compared to previous years (Table 4). The same low or negative NEP values were also evident during periods of low water levels in Pond 3 during

2015 and 2016. Pond 6 showed much less variations in water depth over time and did not exhibit the same low GPP and R values as the desiccating ponds.

Discussion:

Influence of extreme drought on ponds

The Scandinavian 2018 summer was extremely dry as is evident from satellite imagery (Fig. 1). If one disregards the last days of August, the precipitation was the lowest observed over the last 100 years on Öland. Combined with air temperatures generally >2 °C warmer than the long term average, shallow freshwater ecosystems with low summer inflow will inevitably be strongly affected. The extremity lies in the early onset and prolonged duration of this event, while the meteorological data during the week-long measuring campaigns in June 2017 and 2018 were similar (Fig. S1). The conditions prior to June measurements resulted in very low water level in the investigated ponds which allowed us to examine the importance of CO_2 efflux from air-exposed sediments.

Because the ponds are ephemeral they are often subject to desiccation regulated by climate conditions. However, desiccation usually occurs one-two months later than in 2018 (Christensen et al. 2013). In the face of climate change, events such as those reported here are expected to increase in frequency and duration in the future with projected stronger winter rain as opposed to more frequent summer drought (Bates et al. 2008). Globally, the consequences associated with drought and transitioning of freshwater ecosystems to seasonal or ephemeral stages require attention (Marcé et al. 2019). In a recent temporally resolved inventory of the Earth's surface waters, it was reported that within the last about 30 years, 72.000 km^2 (2.6 % of inland water surfaces) have transitioned from a permanent to a seasonal stage emphasising the substantial area subject to this phenomenon (Pekel et al. 2016).

Environmental drivers of CO_2 effluxes from air-exposed sediments

As expected, we found much higher CO_2 effluxes from recently air-exposed sediments compared to the pond water surface (Fig. 2, hypothesis 1). Only in completely dry sediments with negligible water content, did CO_2 production decrease to undetectable levels (Fig. 3). It is evident that the CO_2 effluxes are at their highest soon after sediments become exposed to air. This response is expected as the water content is high and labile organic matter is present due to the limiting oxygen supply during the falling water level before air exposure (Fig. 6, Table 4; Kosten et al. (2018)). As

the sediments continue to dry out, the efflux rates are regulated by the temperature and water content with water content itself influencing the diel temperature course (Fig. 3 and 4). We found a negative relationship between organic matter content and CO_2 efflux which differs from the positive relationship found in previous studies on ephemeral streams (Gallo et al. 2014) and ponds (Catalán et al. 2014). If the CO_2 efflux is carbon limited, a positive relationship to organic content is anticipated. However, because water content is by far the most important determinant of the CO_2 efflux from desiccating pond sediments, an unknown ecological or statistical interaction may perhaps account for the unexpected relationship. A reduced CO_2 efflux could arise if desiccating organic sediments experience a reduced exchange of oxygen and CO_2 between the overlying air and the pore-waters of high degradation activity.

The tight regulation of the CO_2 efflux by sediment water content is similar to that in warm arid ecosystems (Leon et al. 2014; Vargas et al. 2018). A second peak of efflux may occur once the dry sediment is rewetted suggesting accumulation of intermediary organic products that are finally converted to CO_2 when water conditions improve (Fromin et al. 2010). Rewetting may further stimulate carbon processing by increasing the delivery of dissolved inorganic and organic carbon to surface waters (Kosten et al. 2018). The increased oxygen availability in sediments during air-exposure, which promotes CO_2 production, also stimulates CH_4 oxidation and reduce CH_4 effluxes compared with inundated habitats (Koschorreck 2000). Thus, examination of greenhouse gas emissions from periodically air-exposed sediments in terms of total CO_2 equivalents should be a priority for future research (Grinham et al. 2018).

The pronounced spatial variability between and within sites hampered our ability to resolve the time course of CO_2 effluxes, and upscale our measurements to the entire system delineated by the maximum water covered area. While we were unable to provide reliable estimates of the influence of drying on the whole system carbon budget, the high CO_2 effluxes and fast turnover of the sediment organic carbon pool during air exposure (Table 2) showed that this phenomenon plays a substantial role. The net carbon burial during fluctuating inundation and dry phases is important in the light of climate change, which is expected to influence the hydrological cycle by increasing the frequency and duration of drought (Mishra and Singh 2010) potentially exposing previously inundated organic carbon storages to enhanced degradation in air (Downing et al. 2008; Jin et al. 2016). As the age of our study ponds is known to be approximately 30 years, we can derive at an average carbon deposition rate per year as the mean of the organic carbon contents in the sediments divided by pond age. By using an observed median efflux of 7.6 mmol CO_2 m^{-2} h^{-1}

from air-exposed wet sediments, it would only take an estimated 18 days of air-exposure under moist conditions to respire the net annual carbon deposition. This calculation supports existing studies showing that carbon processing in temporary ponds is substantial even though they are not covered by water and it iterates the need for further studies on these processes (Fromin et al. 2010; Obrador et al. 2018).

The observed sediment CO_2 efflux reflects the CO_2 partial pressure gradients between the sediment air pores and the overlying atmosphere and is driven by microbial CO_2 production. We cannot be certain, however, that there is an exact 1:1 relationship between the measured CO_2 efflux and the microbial CO_2 production. This requires that the combined pools of CO_2 in the air pores and $CO_2 + HCO_3^-$ in the pore water of the sediment either remain constant or undergoes small changes relative to the efflux rate during measurements (Skinner et al. 2014). The constant efflux rates over the measuring period suggest that this is the case. We expect that the CO_2 partial pressures in the small water and air pores in the sediment remain close to equilibrium because of the minute distances, but HCO_3^- pools in the pore water may either increase or decrease as a result of changes in pH and alkalinity. Such changes may, in theory, derive from altered dissolution rates of carbonate (consuming CO_2 and forming HCO_3^-), oxidation of fatty acids (increasing pH and converting CO_2 to HCO_3^-) and pore-water volume. Repeated measurements at same spot during the day may be useful to evaluate the CO_2 efflux-microbial production relationship.

Desiccation in ponds

In previous investigations of these charophyte-dominated ponds we have described a daily recurring inorganic carbon pump (Andersen et al. 2019). During daytime, a thermocline develops and separates the surface and bottom waters lasting until the water surface cools at night and causes vertical mixing (Andersen et al. 2017b). Charophyte photosynthesis is accompanied by daytime calcification and calcium carbonate loss from the surface waters to the bottom waters and sediments, while respiration in bottom waters re-dissolves calcium carbonate and vertical mixing reinjects dissolved calcium and bicarbonate into surface waters and supports subsequent photosynthesis (Andersen et al. 2017a). At high charophyte biomass in June, the net balance of carbonate precipitation and dissolution is close to zero (Andersen et al. 2019) and will have no direct influence on air-water CO_2 exchange despite the essential role of the inorganic carbon pump in driving photosynthesis and associated calcification (Sand-Jensen et al. 2018). Progressive desiccation will likely weaken the diel carbon pump as the water level and photosynthetic rate decrease and the pond is

turned into a net CO_2 source to the atmosphere when charophytes undergo senescence and respiration (R) surpasses gross primary production (GPP).

As we expected (hypothesis 2), GPP and R were generally of lower magnitude in June 2018 and NEP rates were slightly negative or zero compared to previous years with a higher water level in the ponds (Table 4; Martinsen et al. (2017)). The reduced metabolic capacity is likely caused by several factors such as critically high water temperature, reduced water movement and damaged canopy structure by compression in a very shallow water column. The erratic temporal changes in pH and oxygen are likely caused by the negligible water movements within the canopy, mainly occurring during nocturnal convective vertical mixing, while wind driven turbulence is attenuated by the dense canopy (Andersen et al. 2017b). Furthermore, the high pH in the small water volume during several hours each day likely reduces photosynthesis (Christensen et al. 2013). The net CO_2 emission from the water surfaces also points at ongoing vegetation senescence in the ponds. A switch from net CO_2 sink to net CO_2 source during desiccation has also been observed in small experimental ponds (Gilbert et al. 2017).

The simple metabolism model previously used successfully in the same ponds could not adequately reproduce the observed oxygen signal when the model was fitted on data from a single day. Therefore, we used data from several days to estimate the metabolic parameters as this approach is less prone to sudden changes in oxygen. Other alternatives may include smoothing of the oxygen time series, for example using a simple moving averages or a Kalman filter (Batt and Carpenter 2012; Staehr et al. 2010). Another consequence of the restricted mixing could be an underestimation of sediment respiration. However, previous studies in Pond 4 found that the contribution of sediment respiration to total ecosystem respiration was low (~10%; Kragh et al. (2017)) and that the water volume below the diurnal thermocline was small relative to the entire pond volume (Martinsen et al. 2017). These conditions should result in a low bias when estimating ecosystem metabolism despite the simple model applied. Future studies on the influence of physical processes may take advantage of more advanced metabolism models and field measurements of water flow using acoustic Doppler velocimetry (Brothers et al. 2017; Cavalcanti et al. 2016).

Implications for organisms in ponds

Ponds support high biodiversity and many organisms rely on temporary systems for their existence (Biggs et al. 2017; Williams et al. 2004). However, it is remarkable that many organisms can cope with the extreme environmental

conditions including pronounced diurnal variations in these habitats (Fig. 6). Many invertebrates and amphibians (Griffiths 1997) have adapted to life in temporary ponds, but leave the habitat before they desiccate. In addition to these organisms, we observed small individuals of northern pike (*Esox lucius*) in Ponds 4 and 5, which had survived partial desiccation but succumb at complete desiccation. It is surprising that this fish species can survive considering the recurring hypoxia (< 2 mg l^{-1}) combined with high water temperature (up to 28.4 °C in Pond 4; Fig. 6, Casselman and Lewis (1996)) and the increasing hypoxic stress at rising temperatures (Raat 1988). Presumably, northern pike can acclimate to these stressful conditions perhaps by selecting pockets of oxic water within the pond and down-scaling its metabolism.

Conclusions

When small shallow vegetated ponds dry out, organisms within the pond may be challenged as environmental conditions worsen. The submerged macrophyte biomass built up during spring enters a stage of senescence reducing photosynthetic capacity and causing respiration to exceed gross primary production. This development changes the ponds from being net sinks to becoming net sources of CO_2. Considering the periodically air-exposure of sediments, it is noticeable that large quantities of carbon are processed and emitted as CO_2 into the atmosphere. Because heatwaves and irregular precipitation are expected to become more prominent in a future climate, the influence of altering hydrology on carbon processing in inland waters is a research theme, which requires more attention.

References:

Abril G et al. (2015) Large overestimation of pCO2 calculated from pH and alkalinity in acidic, organic-rich freshwaters Biogeosciences 12:67-78 doi:10.5194/bg-12-67-2015

Andersen MR, Kragh T, Martinsen KT, Kristensen E, Sand-Jensen K (2019) The carbon pump supports high primary production in a shallow lake Aquat Sci 81:24 doi:10.1007/s00027-019-0622-7

Andersen MR, Kragh T, Sand-Jensen K (2017a) Extreme diel oxygen and carbon cycles in shallow vegetated lakes Proceedings of the Royal Society B 284:20171427 doi:10.1098/rspb.2017.1427

Andersen MR, Sand-Jensen K, Iestyn Woolway R, Jones ID (2017b) Profound daily vertical stratification and mixing in a small, shallow, wind-exposed lake with submerged macrophytes Aquat Sci 79:395-406 doi:10.1007/s00027-016-0505-0

Barko JW, Smart RM (1986) Sediment-related mechanisms of growth limitation in submersed macrophytes Ecology 67:1328-1340 doi:10.2307/1938689

Barton K (2018) MuMIn: Multi-Model Inference, R package version 1.40.4. https://CRAN.R-project.org/package=MuMIn.

Bastviken D, Sundgren I, Natchimuthu S, Reyier H, Gålfalk M (2015) Technical Note: Cost-efficient approaches to measure carbon dioxide (CO 2) fluxes and concentrations in terrestrial and aquatic environments using mini loggers Biogeosciences 12:3849-3859 doi:10.5194/bg-12-3849-2015

Bates BC, Kundzewicz ZW, Wu S, Palutikof JP (2008) Climate Change and Water. Technical Paper of the Intergovernmental Panel on Climate Change, IPCC Secretariat. World Health Organization, Geneva

Bates D, Mächler M, Bolker B, Walker S (2015) Fitting Linear Mixed-Effects Models Using lme4 Journal of Statistical Software 67 doi:10.18637/jss.v067.i01

Batt RD, Carpenter SR (2012) Free-water lake metabolism: addressing noisy time series with a Kalman filter Limnol Oceanogr Methods 10:20-30 doi:10.4319/lom.2012.10.20

Biggs J, von Fumetti S, Kelly-Quinn M (2017) The importance of small waterbodies for biodiversity and ecosystem services: implications for policy makers Hydrobiologia 793:3-39 doi:10.1007/s10750-016-3007-0

Bolker BM, Brooks ME, Clark CJ, Geange SW, Poulsen JR, Stevens MHH, White J-SS (2009) Generalized linear mixed models: a practical guide for ecology and evolution Trends Ecol Evol 24:127-135 doi:10.1016/j.tree.2008.10.008

Brothers S, Kazanjian G, Köhler J, Scharfenberger U, Hilt S (2017) Convective mixing and high littoral production established systematic errors in the diel oxygen curves of a shallow, eutrophic lake Limnol Oceanogr Methods 15:429-435 doi:10.1002/lom3.10169

Burnham KP, Anderson DR (2002) Model Selection and Multimodel Inference: A Practical Information-Theoretic Approach. Springer, New York

Baastrup-Spohr L, Kragh T, Petersen K, Moeslund B, Schou JC, Sand-Jensen K (2016) Remarkable richness of aquatic macrophytes in 3-years old re-established Lake Fil, Denmark Ecol Eng 95:375-383 doi:10.1016/j.ecoleng.2016.06.081

Baastrup-Spohr L, Møller CL, Sand-Jensen K (2016) Water-level fluctuations affect sediment properties, carbon flux and growth of the isoetid Littorella uniflora in oligotrophic lakes Freshwat Biol 61:301-315 doi:10.1111/fwb.12704

Casselman JM, Lewis CA (1996) Habitat requirements of northern pike (Essox lucius) Can J Fish Aquat Sci 53:161-174 doi:10.1139/f96-019

Catalán N, von Schiller D, Marcé R, Koschorreck M, Gomez-Gener L, Obrador B (2014) Carbon dioxide efflux during the flooding phase of temporary ponds Limnetica 33:349-360

Cavalcanti JR, da Motta-Marques D, Fragoso Jr CR (2016) Process-based modeling of shallow lake metabolism: Spatio-temporal variability and relative importance of individual processes Ecol Model 323:28-40 doi:10.1016/j.ecolmodel.2015.11.010

Christensen J, Sand-Jensen K, Staehr PA (2013) Fluctuating water levels control water chemistry and metabolism of a charophyte-dominated pond Freshwat Biol 58:1353-1365 doi:10.1111/fwb.12132

Cole JJ et al. (2007) Plumbing the global carbon cycle: integrating inland waters into the terrestrial carbon budget Ecosystems 10:172-185 doi:10.1007/s10021-006-9013-8

Downing J et al. (2006) The global abundance and size distribution of lakes, ponds, and impoundments Limnol Oceanogr 51:2388-2397 doi:10.4319/lo.2006.51.5.2388

Downing JA et al. (2008) Sediment organic carbon burial in agriculturally eutrophic impoundments over the last century Global Biogeochemical Cycles 22 doi:10.1029/2006gb002854

Fromin N, Pinay G, Montuelle B, Landais D, Ourcival J, Joffre R, Lensi R (2010) Impact of seasonal sediment desiccation and rewetting on microbial processes involved in greenhouse gas emissions Ecohydrology 3:339-348 doi:10.1002/eco.115

Gallo EL, Lohse KA, Ferlin CM, Meixner T, Brooks PD (2014) Physical and biological controls on trace gas fluxes in semi-arid urban ephemeral waterways Biogeochemistry 121:189-207 doi:10.1007/s10533-013-9927-0

Gilbert PJ, Cooke DA, Deary M, Taylor S, Jeffries MJ (2017) Quantifying rapid spatial and temporal variations of CO2 fluxes from small, lowland freshwater ponds Hydrobiologia 793:83-93 doi:10.1007/s10750-016-2855-y

Gómez-Gener L et al. (2016) When Water Vanishes: Magnitude and Regulation of Carbon Dioxide Emissions from Dry Temporary Streams Ecosystems 19:710-723 doi:10.1007/s10021-016-9963-4

Gómez-Gener L et al. (2015) Hot spots for carbon emissions from Mediterranean fluvial networks during summer drought Biogeochemistry 125:409-426 doi:10.1007/s10533-015-0139-7

Gran G (1952) Determination of the equivalence point in potentiometric titrations. Part II Analyst 77:661-671 doi:10.1039/an9527700661

Griffiths RA (1997) Temporary ponds as amphibian habitats Aquat Conserv: Mar Freshwat Ecosyst 7:119-126

Grinham A et al. (2018) The importance of small artificial water bodies as sources of methane emissions in Queensland, Australia Hydrology and Earth System Sciences 22:5281-5298 doi:10.5194/hess-2018-294

Hecnar SJ, M'Closkey RT (1997) The effects of predatory fish on amphibian species richness and distribution Biol Conserv 79:123-131 doi:10.1016/s0006-3207(96)00113-9

Holgerson MA, Raymond PA (2016) Large contribution to inland water CO2 and CH4 emissions from very small ponds Nature Geoscience 9:222-226 doi:10.1038/ngeo2654

Jassby AD, Platt T (1976) Mathematical formulation of the relationship between photosynthesis and light for phytoplankton Limnol Oceanogr 21:540-547 doi:10.4319/lo.1976.21.4.0540

Jin H, Yoon TK, Lee S-H, Kang H, Im J, Park J-H (2016) Enhanced greenhouse gas emission from exposed sediments along a hydroelectric reservoir during an extreme drought event Environmental Research Letters 11:124003 doi:10.1088/1748-9326/11/12/124003

Jørgensen SE, Bendoricchio G (2001) Fundamentals of ecological modelling vol 21. Developments in environmental modelling. Elsevier, Amsterdam

Koschorreck M (2000) Methane turnover in exposed sediments of an Amazon floodplain lake Biogeochemistry 50:195-206 doi:10.1023/A:1006326018597

Kosten S et al. (2018) Extreme drought boosts CO2 and CH4 emissions from reservoir drawdown areas Inland Waters 8:329-340 doi:10.1080/20442041.2018.1483126

Kragh T, Andersen MR, Sand-Jensen K (2017) Profound afternoon depression of ecosystem production and nighttime decline of respiration in a macrophyte-rich, shallow lake Oecologia 185:157-170 doi:10.1007/s00442-017-3931-3

Leon E, Vargas R, Bullock S, Lopez E, Panosso AR, La Scala N (2014) Hot spots, hot moments, and spatio-temporal controls on soil CO2 efflux in a water-limited ecosystem Soil Biol Biochem 77:12-21 doi:https://doi.org/10.1016/j.soilbio.2014.05.029

Lloyd J, Taylor J (1994) On the temperature dependence of soil respiration Funct Ecol 8:315-323 doi:10.2307/2389824

Marcé R et al. (2019) Emissions from dry inland waters are a blind spot in the global carbon cycle Earth-Sci Rev 188:240-248 doi:10.1016/j.earscirev.2018.11.012

Martinsen KT, Andersen MR, Kragh T, Sand-Jensen K (2017) High rates and close diel coupling of primary production and ecosystem respiration in small, oligotrophic lakes Aquat Sci 79:995-1007 doi:10.1007/s00027-017-0550-3

Martinsen KT, Andersen MR, Sand-Jensen K (2019) Water temperature dynamics and the prevalence of daytime stratification in small temperate shallow lakes Hydrobiologia 826:247-262 doi:10.1007/s10750-018-3737-2

Martinsen KT, Kragh T, Sand-Jensen K (2018) Technical note: A simple and cost-efficient automated floating chamber for continuous measurements of carbon dioxide gas flux on lakes Biogeosciences 15:5565-5573 doi:10.5194/bg-15-5565-2018

Mendonça R, Müller RA, Clow D, Verpoorter C, Raymond P, Tranvik LJ, Sobek S (2017) Organic carbon burial in global lakes and reservoirs Nature Communications 8:1694 doi:10.1038/s41467-017-01789-6

Mishra AK, Singh VP (2010) A review of drought concepts Journal of Hydrology 391:202-216 doi:10.1016/j.jhydrol.2010.07.012

Nakagawa S, Schielzeth H (2013) A general and simple method for obtaining R2 from generalized linear mixed-effects models Methods in Ecology and Evolution 4:133-142 doi:10.1111/j.2041-210x.2012.00261.x

Obrador B, von Schiller D, Marcé R, Gómez-Gener L, Koschorreck M, Borrego C, Catalán N (2018) Dry habitats sustain high CO 2 emissions from temporary ponds across seasons Scientific Reports 8:3015 doi:10.1038/s41598-018-20969-y

Pekel J-F, Cottam A, Gorelick N, Belward AS (2016) High-resolution mapping of global surface water and its long-term changes Nature 540:418-422 doi:10.1038/nature20584

Prairie YT et al. (2018) Greenhouse gas emissions from freshwater reservoirs: what does the atmosphere see? Ecosystems 21:1058-1071 doi:10.1007/s10021-017-0198-9

R Core Team (2018) R: A language and environment for statistical computing. Vienna, R Foundation for Statistical Computing.

Raich JW, Schlesinger WH (1992) The global carbon dioxide flux in soil respiration and its relationship to vegetation and climate Tellus B 44:81-99 doi:10.1034/j.1600-0889.1992.t01-1-00001.x

Raymond PA et al. (2013) Global carbon dioxide emissions from inland waters Nature 503:355-359 doi:10.1038/nature12760

Read JS et al. (2011) Derivation of lake mixing and stratification indices from high-resolution lake buoy data Environ Model Software 26:1325-1336 doi:10.1016/j.envsoft.2011.05.006

Raat AJ (1988) Synopsis of biological data on the northern pike: Esox lucius Linnaeus, 1758. FAO Fish. Synop., (30) Rev. 2.

Sand-Jensen K, Båstrup-Spohr L, Andersen MR, Christensen JPA, Alnoee AB, Jespersen TS (2015) Mellan torka och översvämning på Öland Sven Bot Tidskr 109

Sand-Jensen K et al. (2018) Photosynthesis and calcification of charophytes Aquat Bot 149:46-51 doi:10.1016/j.aquabot.2018.05.005

Sand-Jensen K, Pedersen MF, Nielsen SL (1992) Photosynthetic use of inorganic carbon among primary and secondary water plants in streams Freshwat Biol 27:283-293 doi:10.1111/j.1365-2427.1992.tb00540.x

Sand-Jensen K, Møller CL (2014) Reduced root anchorage of freshwater plants in sandy sediments enriched with fine organic matter Freshwat Biol 59:427-437 doi:10.1111/fwb.12275

Sand-Jensen K, Pedersen NL, Søndergaard M (2007) Bacterial metabolism in small temperate streams under contemporary and future climates Freshwat Biol 52:2340-2353

Schiller Dv, Marcé R, Obrador B, Gómez-Gener L, Casas-Ruiz JP, Acuña V, Koschorreck M (2014) Carbon dioxide emissions from dry watercourses Inland waters 4:377-382

Skinner D, Oliver R, Aldridge K, Brookes J (2014) Extreme water level decline effects sediment distribution and composition in Lake Alexandrina, South Australia Limnology 15:117-126 doi:10.1007/s10201-013-0422-z

This is a post-peer-review, pre-copyedit version of an article published in Biogeochemistry. The final authenticated version is available online at: https://doi.org/10.1007/s10533-019-00579-0

SMHI (2018) Swedish Meteorological and Hydrological Institute. http://www.smhi.se/klimatdata. Accessed February 2019

Solomon CT et al. (2013) Ecosystem respiration: drivers of daily variability and background respiration in lakes around the globe Limnol Oceanogr 58:849-866 doi:10.4319/lo.2013.58.3.0849

Staehr PA et al. (2010) Lake metabolism and the diel oxygen technique: state of the science Limnol Oceanogr Methods 8:628-644 doi:10.4319/lom.2010.8.0628

Taylor S, Gilbert PJ, Cooke DA, Deary ME, Jeffries MJ (2019) High carbon burial rates by small ponds in the landscape Front Ecol Environ 17:25-31 doi:doi:10.1002/fee.1988

Tranvik LJ et al. (2009) Lakes and reservoirs as regulators of carbon cycling and climate Limnol Oceanogr 54:2298-2314 doi:10.4319/lo.2009.54.6_part_2.2298

Vargas R, Sánchez-Cañete P. E, Serrano-Ortiz P, Curiel Yuste J, Domingo F, López-Ballesteros A, Oyonarte C (2018) Hot-Moments of Soil CO2 Efflux in a Water-Limited Grassland Soil Systems 2:47 doi:10.3390/soilsystems2030047

Verpoorter C, Kutser T, Seekell DA, Tranvik LJ (2014) A global inventory of lakes based on high-resolution satellite imagery Geophys Res Lett 41:6396-6402 doi:10.1002/2014gl060641

Wantzen KM, Rothhaupt K-O, Mörtl M, Cantonati M, László G, Fischer P (2008) Ecological effects of water-level fluctuations in lakes: an urgent issue Hydrobiologia 613:1-4 doi:10.1007/978-1-4020-9192-6_1

Weise L et al. (2016) Water level changes affect carbon turnover and microbial community composition in lake sediments FEMS Microbiol Ecol 92:fiw035 doi:10.1093/femsec/fiw035

Weyhenmeyer GA, Kortelainen P, Sobek S, Müller R, Rantakari M (2012) Carbon dioxide in boreal surface waters: a comparison of lakes and streams Ecosystems 15:1295-1307 doi:10.1007/s10021-012-9585-4

Williams DD (1997) Temporary ponds and their invertebrate communities Aquat Conserv: Mar Freshwat Ecosyst 7:105-117

Williams P, Whitfield M, Biggs J, Bray S, Fox G, Nicolet P, Sear D (2004) Comparative biodiversity of rivers, streams, ditches and ponds in an agricultural landscape in Southern England Biol Conserv 115:329-341 doi:10.1016/s0006-3207(03)00153-8

This is a post-peer-review, pre-copyedit version of an article published in Biogeochemistry. The final authenticated version is available online at: https://doi.org/10.1007/s10533-019-00579-0

Figure captions:

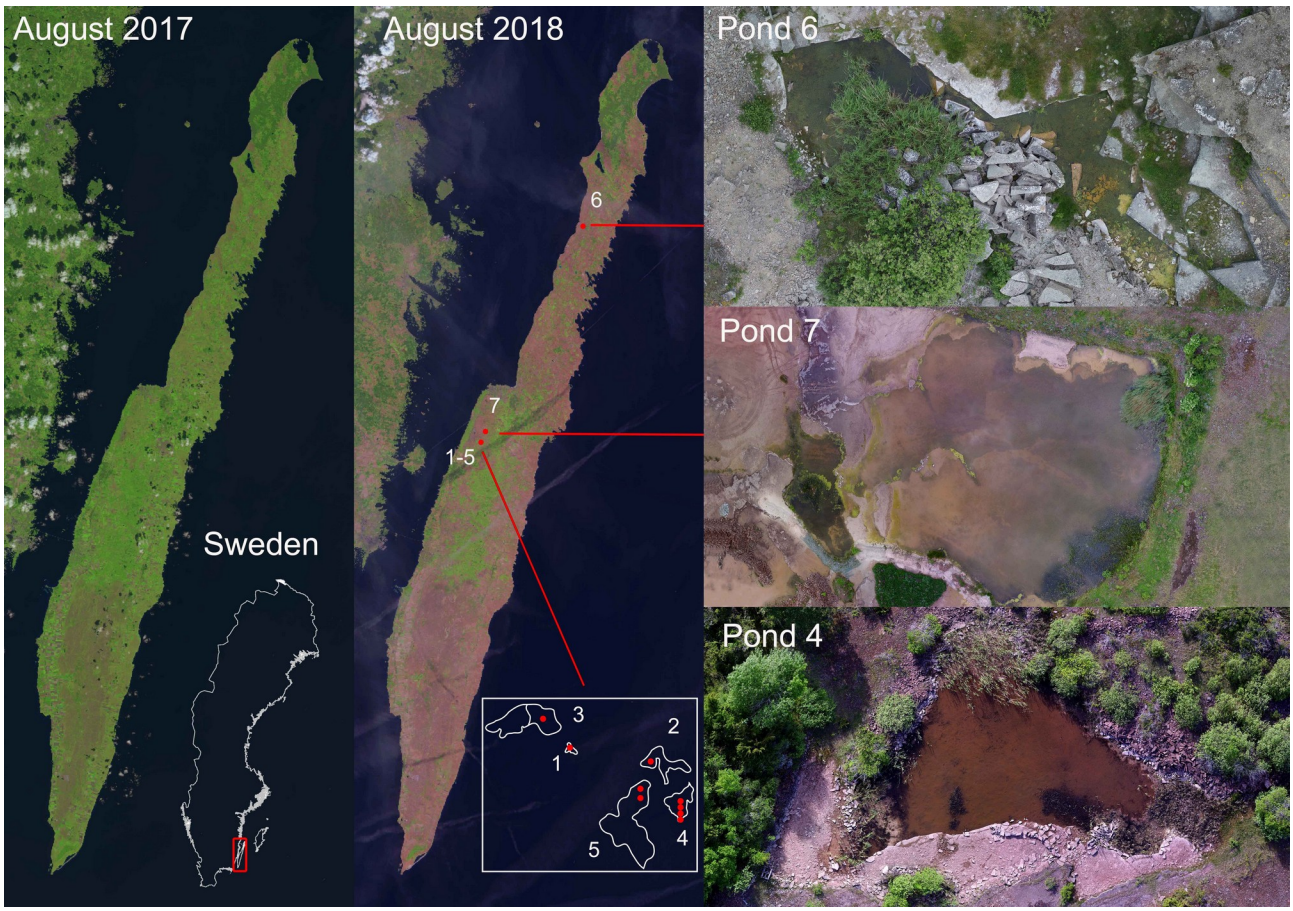

Fig. 1 Landsat satellite imagery (Landsat-8 image courtesy of the U.S. Geological Survey), map of the study area and drone images of three investigated ponds. From left to right: satellite image of Öland during August 2017 (left) and 2018 (middle) along with drone imagery from three ponds (right). Also included, is an insert map of Ponds 1 to 5 (middle) where CO_2 effluxes from air-exposed sediments were measured (red dots). Drone imagery was recorded during 2017

This is a post-peer-review, pre-copyedit version of an article published in Biogeochemistry. The final authenticated version is available online at: https://doi.org/10.1007/s10533-019-00579-0

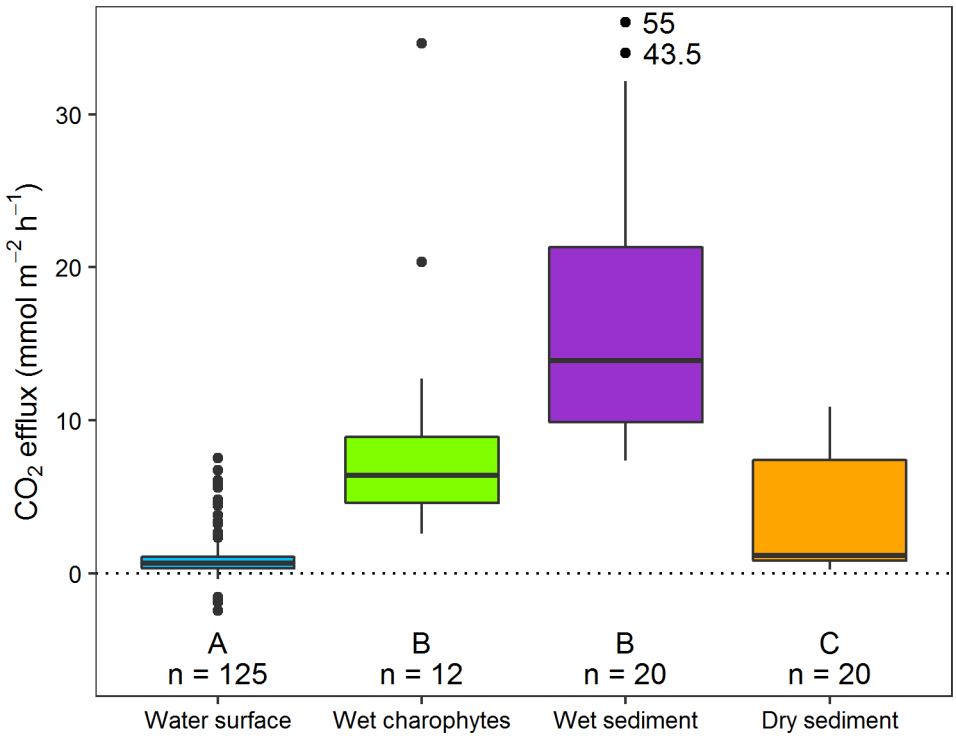

Fig. 2 Comparison of CO_2 efflux measured during summer 2018 (mmol m^{-2} h^{-1}) between habitats (see text) with box-plots showing median (solid horizontal line), 25% and 75% quartile (upper and lower hinge), lines extending to one and a half times the inter-quartile range (upper and lower whisker) and observations outside this range (points). Number of observations (n) and statistical differences between groups have different letters (A, B and C, $p<0.05$, Kruskal-Wallis test with Dunn's test for multiple comparisons)

This is a post-peer-review, pre-copyedit version of an article published in Biogeochemistry. The final authenticated version is available online at: https://doi.org/10.1007/s10533-019-00579-0

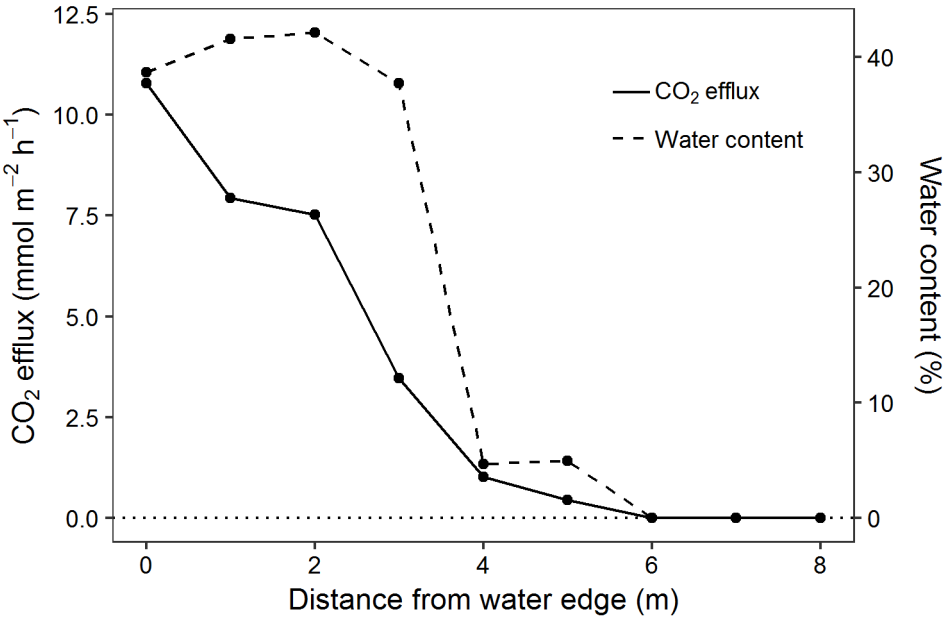

Fig. 3 Sediment CO_2 efflux measured during summer 2018 (solid line) and water content (dashed line) measured along a natural moisture gradient from the water edge to eight meters away (Pond 5). Mean values of two replicates

This is a post-peer-review, pre-copyedit version of an article published in Biogeochemistry. The final authenticated version is available online at: https://doi.org/10.1007/s10533-019-00579-0

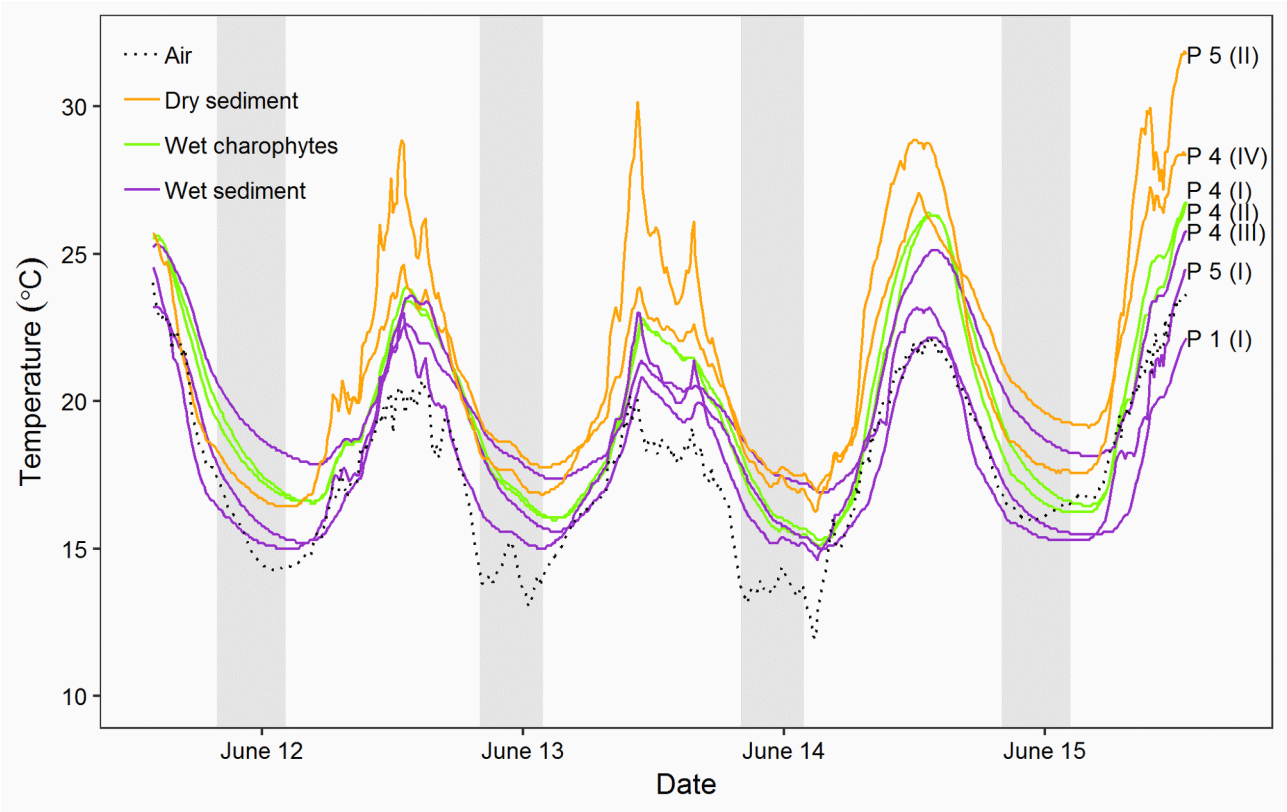

Fig. 4 Temperature in air-exposed sediments measured during summer 2018 at seven sites (P1-P5) with different sediment status (different line colours) accompanying CO_2 efflux measurements and air temperature (dotted line). Grey boxes indicate night-time

This is a post-peer-review, pre-copyedit version of an article published in Biogeochemistry. The final authenticated version is available online at: https://doi.org/10.1007/s10533-019-00579-0

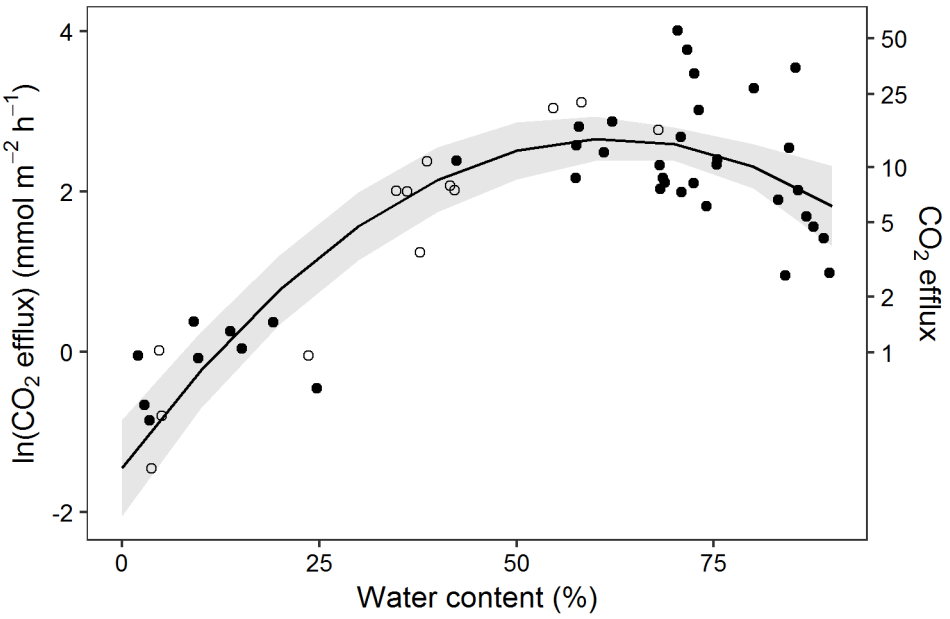

Fig. 5 Relationship between sediment CO_2 efflux (ln-transformed primary y-axis and original scale on secondary y-axis) and water content (x-axis) as fitted from the linear mixed-effect model (solid line) and 95% confidence intervals (grey area). Filled points are observations used to fit the model (Table 3) and open points are data points where sediment temperatures were not measured and included in the model

This is a post-peer-review, pre-copyedit version of an article published in Biogeochemistry. The final authenticated version is available online at: https://doi.org/10.1007/s10533-019-00579-0

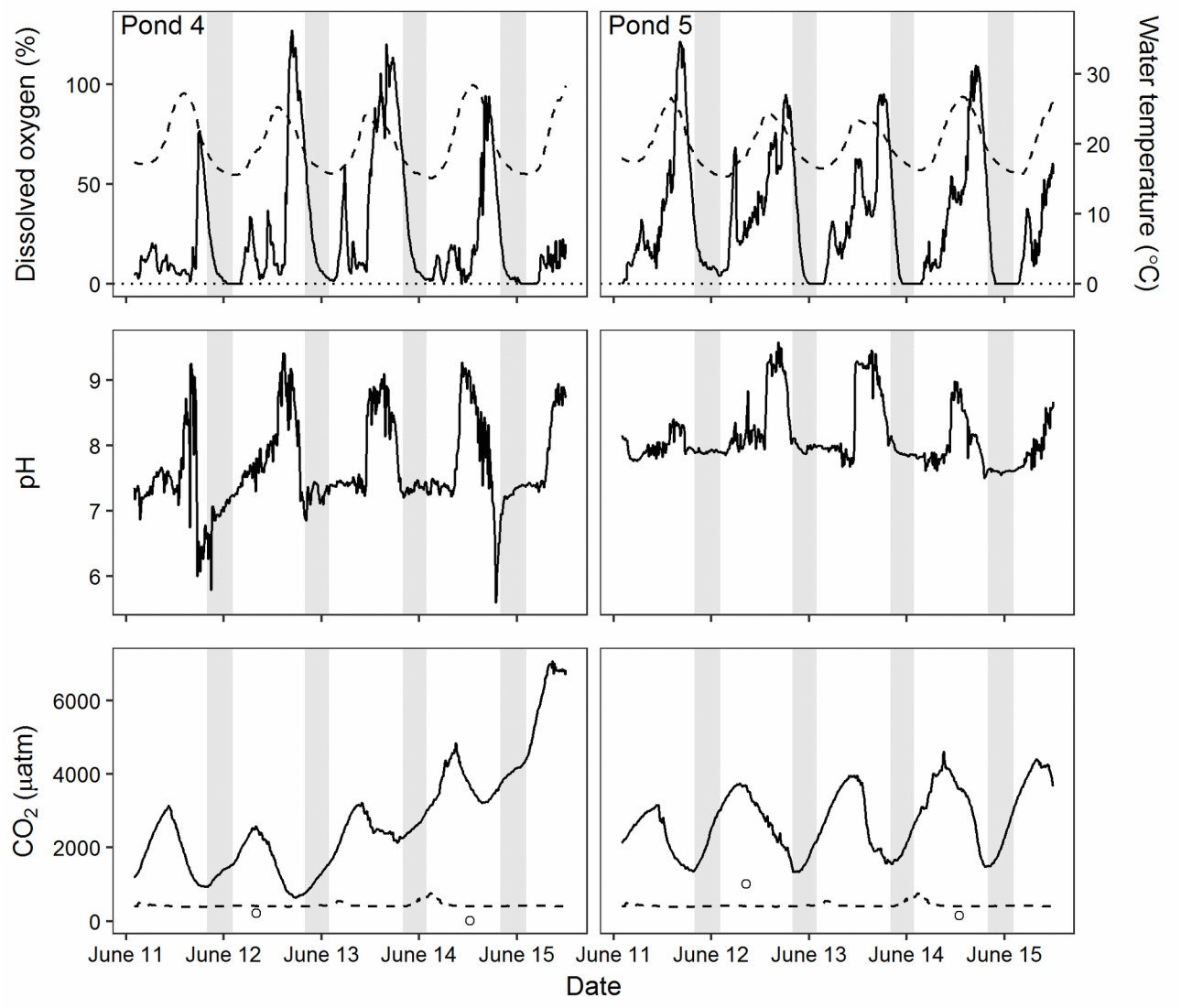

Fig. 6 Upper panels: Dissolved oxygen (% air saturation) and water temperature (secondary y-axis, dashed line). Middle panels: water pH. Lower panels: CO_2 partial pressure (µatm) measured in a permanent floating chamber (solid line), CO_2 partial pressure in air (µatm, dashed line) and water side CO_2 partial pressure estimated from alkalinity, pH and water temperature (µatm, open points). Measurements are from summer 2018 in Pond 4 and 5. Grey boxes indicate night-time

This is a post-peer-review, pre-copyedit version of an article published in Biogeochemistry. The final authenticated version is available online at: https://doi.org/10.1007/s10533-019-00579-0

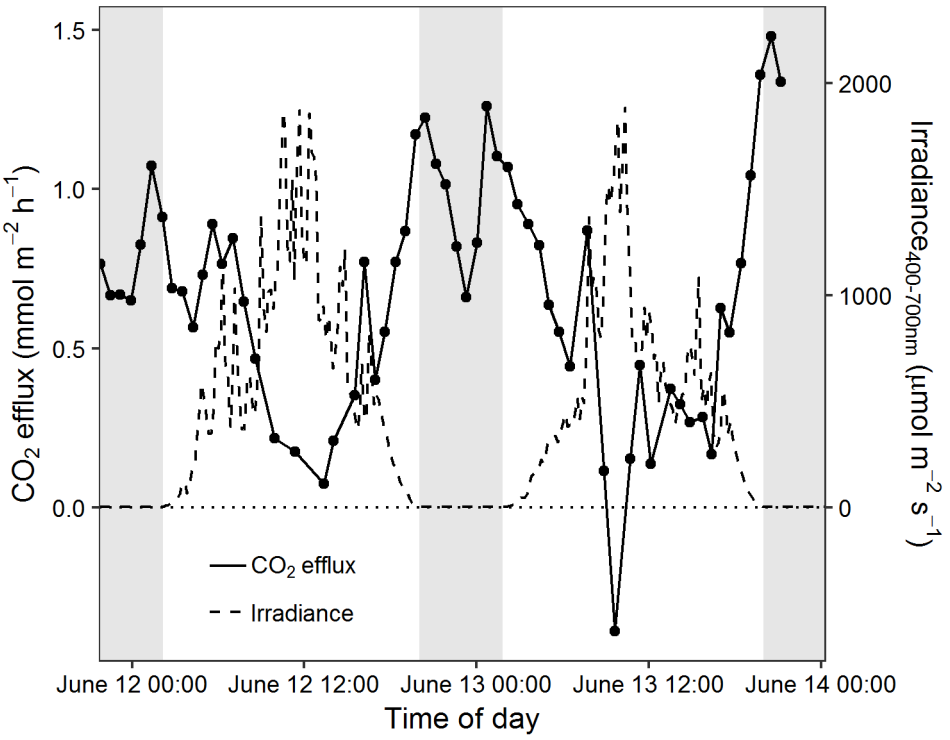

Fig. 7 Continuous measurements of CO_2 efflux (filled points) and incident irradiance (PAR 400-700 nm, dashed line, secondary y-axis) during two days in summer 2018 on Pond 4. Grey boxes indicate night-time

Table 1. Overview of measurements from the investigated sites during 2017 and 2018.

Year	Period	Site	Measurements
2017	June 12-17	Pond 6, 7	Metabolism; water CO_2 flux
2018	June 11-16	Pond 1	Metabolism; water CO_2 flux
		Pond 4, 5	Metabolism; water CO_2 flux; pH; CO_2 partial pressure
		Pond 1, 6	Metabolism
		Pond 1 (I), 4 (I, II, III, IV), 5 (I, II)	Sediment CO_2 flux; sediment samples; sediment temperature
		Pond 2, 3, 5[a]	Sediment CO_2 flux; sediment samples

[a] Additional measurements in Pond 5 along a wet-dry gradient every 1 meter.

Table 2. Sediment properties and CO_2 efflux and turnover time of organic carbon pool at the investigated nine sites measured during summer 2018. Sediment status: wet or dry (threshold: 50 % water content) and with or without *Chara*. Other sediment characteristics: water content, sediment depth and content of organic matter (LOI_{550}) and carbonates (LOI_{950}) in upper 1 cm layer. Mean values, SD and number of replicates in parenthesis.

Site (units)	Wet area (%)	State	Distance from water edge (m)	Water content (%)	Depth (cm)	LOI_{550} (g m^{-2} cm^{-1})	LOI_{950} (g m^{-2} cm^{-1})	CO_2 efflux (mmol m^{-2} h^{-1})	Turnover (days)
Pond 1 (I)[a]	84	Wet sed.	0.4	73.8 (±3.5, 6)	13.4 (±2.3, 8)	299.2 (±54.1, 6)	781.6 (±87.6, 6)	29.3 (±18.4, 6)	190
Pond 2	0	Dry sed.		41.5 (±14.5, 5)	6.3 (±2.7, 8)	663.8 (±202.7, 5)	632.6 (±118.1, 5)	11.9 (±9.4, 5)	488
Pond 3	0	Dry sed.		15.2 (±29.5, 5)	4.8 (±3.1, 8)	444.5 (±134.7, 5)	879.7 (±434.3, 5)	8.1 (±11.1, 2)	366
Pond 4 (I)[a]	35	Wet *Chara*	0	81.4 (±6.1, 6)	15.4 (±1.2, 8)	331.7 (±43.5, 6)	306.4 (±42.6, 6)	9.1 (±6.4, 6)	780
Pond 4 (II)[a]		Wet *Chara*	1.1	83.9 (±8, 6)	15.5 (±2.3, 8)	357.8 (±119.3, 6)	313.6 (±135.2, 6)	10.1 (±12.2, 6)	763
Pond 4 (III)[a]		Wet sed.	2.4	66.3 (±5.5, 6)	5.4 (±2.3, 8)	413.5 (±83, 6)	660.4 (±125.1, 6)	11.6 (±3.6, 6)	267
Pond 4 (IV)[a]		Dry sed.	3.7	8.7 (±6.1, 5)	1.9 (±0.6, 8)	422.1 (±135.3, 5)	793.7 (±270.2, 5)	0.9 (±0.3, 5)	1238
Pond 5 (I)[a]	26	Wet sed.	1.0	60.7 (±11.3, 6)	2.8 (±0.8, 8)	494.1 (±222.3, 6)	683.9 (±451.5, 6)	11.6 (±3.4, 6)	166
Pond 5 (II)[a]		Dry sed.	2.5	10.6 (±9.4, 6)	2.1 (±0.6, 8)	632.1 (±135.5, 6)	1300.4 (±301.3, 6)	1 (±0.5, 4)	1844

[a] Denotes sites where temperature was also measured and used in the linear-mixed model.

Table 3. Linear mixed-model analysis for predicting CO_2 efflux from air-exposed sediments (ln-transformed, n= 39). The table includes models within four AIC_c units of the best model along with the full model (all parameters included) and null model (intercept only). The table shows parameter estimates with standard errors in parenthesis, R^2_{marg}, R^2_{cond}, number of variables (K), log-likelihood (LL), AIC_c, ΔAIC_c and Akaike weights (ω) for each model.

Model (units)	Intercept (mmol m^{-2} h^{-1})	Temp. (°C)	Water cont. (%)	(Water cont.)^2 ($\%^2$)	Depth (cm)	LOI_{550} (kg m^{-2} cm^{-1})	LOI_{950} (kg m^{-2} cm^{-1})	R^2_{marg}	R^2_{cond}	K	AIC_c	Δ_i	ω_i
Temp. + Water + LOI_{550} + LOI_{950}	-3.1 (1.1)	0.12 (0.032)	0.13 (0.014)	-0.0011 (0.00015)		-5.1 (1.2)	1.4 (0.49)	0.84	0.84	8	77	0	0.55
Full	-2.8 (1.1)	0.13 (0.032)	0.13 (0.014)	-0.00097 (0.00018)	-0.036(0.032)	-6 (1.5)	1.5 (0.49)	0.85	0.85	9	79	2.2	0.19
Temp. + Water + LOI_{550}	-2.3 (1.3)	0.12 (0.031)	0.12 (0.017)	-0.001 (0.00018)		-3.4 (1.7)		0.79	0.84	7	80	2.7	0.14
Temp. + Water	-4.1 (0.92)	0.13 (0.031)	0.12 (0.019)	-0.00091 (0.00019)				0.74	0.83	6	80	3	0.12
Null	1.7 (0.45)							0	0.78	3	100	23	0

Table 4. Ecosystem metabolism (GPP, NEP and R), oxygen saturation, water temperature, surface area, mean depth (z_{mean}) in the investigated ponds during 2017 and 2018 along with previously published data from 2015 and 2016 ([a], Martinsen et al. (2017)). Previous measurements of metabolism are estimated every day while the 2017 and 2018 estimates are calculated based on multiple days (see duration). Dissolved oxygen saturation, water temperature, z_{mean} and metabolism estimates from 2015 and 2016 are reported as means with ranges in parenthesis. Metabolism estimates from 2017 and 2018 are reported as the estimated values and 95 % confidence interval in parenthesis.

Site (units)	Year	Duration (days)	Area (m^2)	z_{mean} (m)	GPP	NEP ($g\ O_2\ m^{-2}\ day^{-1}$)	R	Dissolved oxygen (%)	Water temperature (°C)
Pond 1	2015[a]	4	81	0.22	11 (9.3-14)	1.8 (0.1-3.6)	-9.2 (7-13.9)	121 (24-243)	18.6 (10.4-30.7)
Pond 3		4	340	0.05	1.2 (0.9-1.7)	-0.5 (-0.8--0.2)	-1.7 (1.3-2.1)	67 (12-115)	18 (9.2-31.5)
Pond 4		63	855	0.25	3.3 (0.4-7.4)	0.4 (-0.4-2)	-2.9 (0.5-7.3)	110 (57-187)	12.2 (2.9-24.3)
Pond 5		63	2158	0.17	2.2 (0.4-4.9)	0.1 (-0.2-0.7)	-2.2 (0.5-4.6)	104 (39-169)	11.6 (2.4-23.7)
Pond 1	2016[a]	9	85	0.3	14.2 (11.8-16.4)	2.3 (0.6-4.8)	-11.8 (8.7-14.6)	121 (30-222)	19.8 (10.6-28.3)
Pond 2		9	311	0.17	12.4 (9.9-15.3)	1.5 (-0.2-2.6)	-10.9 (7.7-14.9)	121 (6-278)	19.9 (8.6-31.6)
Pond 3		9	431	0.12	3.4 (2.0-4.8)	0.1 (-0.2-0.2)	-3.3 (1.9-4.8)	96 (18-202)	18.8 (8.1-29.7)
Pond 4		10	827	0.31	8.9 (6.0-12.0)	1.8 (0.6-3.6)	-7.1 (3.5-10.2)	119 (44-186)	20.4 (11.7-29.2)
Pond 6	2017	3	91	0.31	11.3 (8.4, 14.5)	0.7	-10.6 (-8.3, -13.4)	125 (53-210)	17 (14.3-20)
Pond 7		3.8	4841	0.22	2.4 (1.4, 3.9)	0.4	-2 (-1.4, -2.8)	111 (74-147)	19.1 (14-26.1)
Pond 1	2018	3.6	71	0.11	1.8 (0, 3.2)	0	-1.8 (0, -2.9)	30 (0-104)	20.5 (13.8-30.8)
Pond 4		4.9	353	0.09	1.8 (0.8, 32.5)	-0.4	-2.2 (-1.2, -3.3)	28 (0-127)	20.1 (13.8-33.4)
Pond 5		4.9	780	0.17	1.4 (0, 154.6)	-1.2	-2.6 (-1.5, -4.2)	33 (0-121)	20.2 (15.3-27.3)
Pond 6		4.9	91	0.31	7.4 (5.1, 11.1)	-0.2	-7.6 (-6.2, -8.9)	77 (8-173)	19 (16.9-26.6)

Table 5. CO_2 flux from the pond water surface at sites measured during 2017 and 2018 reported as means (±SD, number of determinations).

Site	Year	CO_2 efflux (mmol m^{-2} h^{-1})
Pond 6	2017	0.4 (±0.4, 33)
Pond 7		-1.9 (±0.4, 4)
Pond 1	2018	4.7 (±1.6, 15)
Pond 4		0.7 (±0.4, 66)
Pond 5		1.5 (±0.4, 7)